JOURNAL OF TISSUE ENGINEERING AND REGENERATIVE MEDICINE
J Tissue Eng Regen Med 2014; **8**: 364–376.
Published online 11 June 2012 in Wiley Online Library (wileyonlinelibrary.com) **DOI:** 10.1002/term.1529

RESEARCH ARTICLE

Osteoblastic differentiation and potent osteogenicity of three-dimensional hBMSC-BCP particle constructs

Thomas Cordonnier[1,4], Alain Langonné[2,4], Pierre Corre[5,6], Audrey Renaud[1], Luc Sensebé[2,4], Philippe Rosset[3,4], Pierre Layrolle[1]* and Jérôme Sohier[1]

[1]*Inserm U957, Laboratory for Bone Resorption Physiopathology and Primary Bone Tumour Therapy, Faculty of Medicine, University of Nantes, France*
[2]*Research Department, EFS Centre-Atlantique, Tours, France*
[3]*Departments of Orthopaedic Surgery, University Hospital, François Rabelais University, Tours, France*
[4]*EA3855, Laboratory of Haematopoiesis, University François Rabelais, Tours, France*
[5]*Inserm U791, Laboratory for Osteoarticular and Dental Tissue Engineering, Faculty of Dental Surgery, University of Nantes, France*
[6]*Maxillofacial Departments, CHU Nantes, Hotel-Dieu Hospital, Nantes, France*

Abstract

Bone tissue engineering usually consists of associating osteoprogenitor cells and macroporous scaffolds. This study investigated the *in vitro* osteoblastic differentiation and resulting *in vivo* bone formation induced by a different approach that uses particles as substrate for human bone marrow stromal cells (hBMSCs), in order to provide cells with a higher degree of freedom and allow them to synthesize a three-dimensional (3D) environment. Biphasic calcium phosphate (BCP) particles (35 mg, ~175 μm in diameter) were therefore associated with 4×10^5 hBMSCs. To discriminate the roles of BCP properties and cell-synthesized 3D environments, inert glass beads (GBs) of similar size were used under the same conditions. In both cases, high cell proliferation and extensive extracellular matrix (ECM) production resulted in the rapid formation of thick cell-synthesized 3D constructs. *In vitro*, spontaneous osteoblastic differentiation was observed in the 3D constructs at the mRNA and protein levels by monitoring the expression of Runx2, BMP2, ColI, BSP and OCN. The hBMSC–BCP particle constructs implanted in the subcutis of nude mice induced abundant ectopic bone formation after 8 weeks (~35%, $n = 5/5$). In comparison, only fibrous tissue without bone was observed in the implanted hBMSC–GB constructs ($n = 0/5$). Furthermore, little bone formation (~3%, $n = 5/5$) was found in hBMSC–macroporous BCP discs (diameter 8×3 mm). This study underlines the lack of correspondence between bone formation and *in vitro* differentiation assays. Furthermore, these results highlight the importance of using BCP as well as a 3D environment for achieving high bone yield of interest for bone engineering.

Received 6 April 2011; Revised 9 February 2012; Accepted 3 April 2012

Supporting information may be found in the online version of this article.

Keywords **bone tissue engineering; human bone marrow stromal cells; biphasic calcium phosphate; glass beads; three dimensional constructs; osteoblastic differentiation; osteogenicity in nude mice**

1. Introduction

Each year in the world, millions of patients need treatment for skeletal disorders (Langer and Vacanti, 1993). Many acute and chronic injuries or defects require bone tissue grafting. Bone grafting is a vital component in many surgical procedures to facilitate the repair of bone defects or fusions (Urist and Strates, 1970; Brown and Cruess, 1982; Oklund *et al*., 1986; Damien and Parsons, 1991). Current options include autografts with transplantation of fresh autologous bone or allografts from tissue banks (Burchardt, 1987; Helm *et al*., 2001). However, each of these options has significant limitations, such as the need for a second surgical site, morbidity, limited supply and inadequate size and shape (Johnson *et al*., 1996; LeGeros,

*Correspondence to: Pierre Layrolle, Inserm U957, Faculty of Medicine, 1 Rue Gaston Veil, 44035 Nantes cedex 1, France. E-mail: pierre.layrolle@inserm.fr

2002; Vaccaro, 2002). Bone tissue engineering combining osteoprogenitor cells, synthetic scaffolds and signalling molecules may be an alternative to the conventional biological grafts (Petite *et al*., 2000; Derubeis and Cancedda, 2004).

Mimicking the *in vivo* microenvironment to generate tissues in the laboratory is a major challenge. As a cell source for bone engineering, human bone marrow stromal cells (hBMSCs) have generated great interest. In particular, the multipotency of bone marrow-derived hBMSCs (Friedenstein *et al*., 1976; Prockop, 1997; Pittenger *et al*., 1999) allows for obtaining a high number of osteoblast-derived cells after amplification and differentiation (Bruder *et al*., 1998). On the other hand, the biomaterial scaffold must exhibit appropriate chemistry, morphology and structure to promote cellular adhesion, migration and differentiation of osteoprogenitor cells for the synthesis of new bone tissue. Biphasic calcium phosphate (BCP) ceramics fit well within this profile because these materials mimic natural bone mineral composition, offer bioactivity, osteoconductivity (LeGeros, 2002) and, in some cases, osteoinductivity (Yamasaki and Sakai, 1992; Klein *et al*., 1994; Ripamonti, 1996; Sun *et al*., 2008).

Most of the BCP ceramic formulations used for bone engineering are shaped as porous scaffolds with various pore sizes and porosity to facilitate nutrient and metabolite diffusion cell permeability and bone ingrowth (Ito *et al*., 2004; Okamoto *et al*., 2006; Nair *et al*., 2008). In this approach, hBMSCs are seeded and cultured on the macroporous BCP ceramic, but these constructs induced little bone formation after implantation under the skin of nude mice. This limited quantity of bone formation using hBMSCs cultured on macroporous BCP ceramics may be explained by an insufficient number of osteoprogenitor cells, the dedifferentiation of osteoblastic into fibroblastic cells or a limited vascularization due to an insufficient porosity in the scaffolds. In addition, at the cellular level, ceramic pores (hundreds of micrometers to millimeters) can be considered as two-dimensional (2D) curved surfaces, which differ from the natural three-dimensional (3D) environment occurring during bone formation.

As an alternative to porous scaffolds, ceramic particles of different sizes have been used in conjunction with cells (Krebsbach *et al*., 1997; Fischer *et al*., 2003; Kuznetsov *et al*., 2008; Mankani *et al*., 2008; Zannettino *et al*., 2010). However, in most of these studies, cells mixed with particles were implanted in animal models without prior culture *in vitro*. Recently, we have shown that hBMSCs seeded on biphasic calcium phosphate (BCP) particles (140–200 μm) could proliferate and produce abundant extracellular matrix (ECM) when cultured *in vitro* (Cordonnier *et al*., 2010). Within hours, solid hybrid 3D constructs were formed, composed of BCP particles embedded in a 3D cell-synthesized ECM. Interestingly, unlike the classical bone tissue-engineering approach using macroporous BCP, the *in vitro* culture of cells seeded on BCP particles induced hBMSC osteoblastic differentiation without osteogenic factors. This spontaneous osteoblastic induction raises questions about the respective roles of the 3D environment, cell–cell and cell–scaffold interactions and ECM production in the osteogenicity of hBMSC–scaffold constructs.

The aim of this study was therefore to determine the role of cell-synthesized 3D environments and composition of scaffold in the spontaneous osteoblastic differentiation of hBMSCs *in vitro* as well as to correlate the capacity of these hybrids constructs to form ectopic bone *in vivo*. The osteoblastic differentiation of hBMSCs was determined on 3D constructs obtained using BCP and glass beads (GBs) particles of similar sizes (~175 μm) and on 2D culture on plastic. The osteogenicity of the 3D hybrid constructs was assayed after implantation for 8 weeks under the skin of nude mice and compared to classical macroporous BCP discs used as control.

2. Materials and methods

2.1. Scaffolds

The different scaffolds used in this study are described in Table 1. BCP particles made of hydroxyapatite (20%) and β-tricalcium phosphate (80%), sieved to 140–200 μm, were used (MBCP+®, Biomatlante SA, Vigneux de Bretagne, France). The purity of the BCP particles was analysed by X-ray diffraction (XRD, Philips PW 1830, CuKα source) and Fourier transform infrared spectroscopy (Nicolet, Magna-IR 550). Traces of CaO in the BCP particles were checked by a phenolphthalein test. The surface of BCP particles was measured by mercury intrusion porosimetry (AutoPoreIII, Micromeritics, Verneuil en Halatte,

Table 1. Physicochemical properties of the BCP particles, glass beads and BCP discs used as scaffolds for hMSCs

Scaffold	Composition	Size	Porosity	Surface area (cm^2/g)
BCP particles	HA/β-TCP 20/80	140–200 μm	Microporous intergranular spaces	863 ± 72[a]
Glass beads	SiO_2	150–210 μm	Smooth surface hollow spheres Intergranular spaces	770[b]
Macroporous BCP discs	HA/β-TCP 20/80	Diameter 8 × 3 mm	Macropores of 100–300 μm (10%) Micropores < 10 μm (70%)	323 ± 35[c]

[a]The surface of BCP particles was measured by mercury intrusion porosimetry, with a threshold of 10 μm, in order to eliminate the microporosity that is not accessible to cells ($n = 3$).
[b]The surface of glass beads was calculated from the area of packed spheres with an average diameter of 180 μm.
[c]The surface of macroporous BCP discs was measured by mercury intrusion porosimetry, with a threshold of 10 μm, in order to eliminate the microporosity that is not accessible to cells ($n = 3$).

DOI: 10.1002/term

France) with a threshold of 10 μm and was found to be $863 \pm 72\ cm^2/g$ ($n = 3$). BCP particles were sterilized by beam γ-irradiation (25 kGy). Silicate glass microcarrier beads (GBs) measuring 150–210 μm in diameter were purchased from Sigma-Aldrich (St Louis, MO, USA) and sterilized in an autoclave (Alphaklave23, HMCE, Taillis, France) at 121 °C for 20 min. The surface area of glass beads was deduced from the volume and weight of packed spheres, taking into account a sphere packing density of 65–60% (Reed, 1995) and an average diameter of 180 μm. BCP discs of 75% porosity, 8 mm in diameter and 3 mm in thickness (average weight 0.14 g and pore size 400 μm) were provided by Biomatlante (Cordonnier *et al*., 2011). The chemical composition and surface microstructure of BCP discs and BCP particles were similar as BCP particles were obtained by crushing BCP discs from the same batch. Mercury intrusion porosimetry of the BCP discs indicated a surface area of $323 \pm 35\ cm^2/g$ ($n = 3$, threshold of 10 μm). BCP porous discs were sterilized by γ-irradiation at 25 kGy. The microstructure was observed by scanning electron microscopy (SEM; Leo 1450 VP Carl Zeiss, Oberkochen, Germany) to characterize the shape and surface of the different types of materials. All samples were gold-sputtered before analysis (Denton Vaccum LLC, Desk III, Moorestown, NJ, USA).

2.2. Isolation and *in vitro* expansion of hBMSCs

Mononuclear cells were derived from bone marrow from donors who gave their informed consent for its use, and the protocol was approved by the Tours University Hospital ethics committee (Tours, France). Bone-marrow aspirates were obtained from six healthy donors (three males and three females, aged 56–82 years) during orthopaedic surgical procedures after exposure of the iliac crest. Aspirates of 5–20 ml were harvested by the use of a bone-marrow biopsy needle inserted through the cortical bone and a plastic syringe of 20 cm^3 rinsed with heparin and containing 1 ml heparin (15 000 IU). Bone-marrow cells were resuspended in α-modified Eagle's medium (α-MEM, Invitrogen, Carlsbad, CA, USA) supplemented with 2 mM L-glutamine, 100 U/ml penicillin, 100 U/ml streptomycin, 10% fetal calf serum (FCS; Hyclone, South Logan, UT, USA) and 1 ng/ml fibroblast growth factor-2 (R&D Systems, Minneapolis, MN, USA). Cells were seeded at 1×10^5 mononucleated cells/cm² and cultured in 5% CO_2 humidified atmosphere at 37 °C. Medium was refreshed twice weekly until cells reach 80% confluence. Then, adherent cells were enzymatically removed from the plate by 3 min of incubation in 0.25% trypsin–EDTA (Lonza, Basel, Switzerland) at 37 °C and seeded at 1×10^3 cells/cm² in culture flasks. Multipotency of hBMSCs was determined by culturing in adipogenic, osteogenic and chondrogenic conditions and using specific histochemical staining (Delorme and Charbord, 2007). Human BMSCs were also characterized by their specific CD markers, positive for CD49a, CD73, CD90 and CD105 and negative for CD45 and CD34 (data not shown). The cells were expanded prior use, until passage 2.

2.3. *In vitro* BMSC culture on biomaterial

BCP particles and glass beads (35 mg) were aliquoted in ultra-low-attachment 24-well plates (Corning Life Sciences, Lowell, MA, USA) to prevent cellular adhesion to the plates. This quantity of BCP or GBs uniformly covered the bottom of each well as a monolayer and corresponded to an available surface area of approximately 30 cm^2. To minimize ion release from the ceramic, BCP particles and discs were incubated for 48 h in twice-refreshed proliferation medium (α-MEM, 10% FCS, 1% antibiotic/antimycotic) before cell seeding. A cellular suspension of 500 μl containing either 4.5×10^5 or 7×10^5 hBMSCs was seeded respectively on BCP particles and GBs or on BCP discs (top seeding), giving the same seeding density of 15 000 cells/cm². Cells were then cultured for several days in proliferation or osteogenic medium [proliferation medium supplemented with β-glycerophosphate (10 mM), ascorbic acid-2-phosphate (0.2 mM), dexamethasone (10^{-8} M; all Sigma-Aldrich)]. The culture medium was refreshed every 3 days. As a control, hBMSCs were seeded on 24-well plastic plates and cultured under the same conditions (15 000 cells/cm²) as for BCP particles or GBs.

2.4. Morphological evaluation and cellular proliferation of hBMSC–scaffold constructs

The constructs were observed by SEM (Leo VP 1450) after dehydratation and metallization. Briefly, samples obtained after 1, 10 and 21 days of culture were dehydrated in successive and increasing ethanol baths and then in increasing grades of 1,1,2-trichloro-1,2,2 trifluoroethane. Samples were then sputtered with a thin layer of gold–palladium (Denton Vacuum, UK) prior to SEM observations.

Cell proliferation was monitored by Alamar blue assay. At different times (days 1, 4, 7, 14 and 21), hBMSC–scaffold constructs in triplicate were washed in phosphate-buffered saline (PBS, 1×; Lonza) before incubation for 45 min at 37 °C and 5% CO_2 in PBS 1× solution containing 10% v/v Alamar blue (BioSource, Caramillo, CA, USA). Acellular scaffolds in duplicates for each type were used to determine a baseline level. For each sample, 200 μl was collected in duplicate and transferred to a 96-well plate before measurement by a fluorescent reader (excitation 530 nm and emission 600 nm; Tristar LB 941, Berthold Technologies, Bad Wildbad, Germany). Microscopy evaluation of cell proliferation involved use of Live/Dead® cell viability assays (Invitrogen) after 1 and 7 days of culture in proliferation medium. hBMSC–scaffold constructs were washed with PBS 1× before incubation for 30 min at 37 °C and 5% CO_2 in 500 μl of a solution containing 0.5 μM calcein AM and 2 μM ethidium

DOI: 10.1002/term

homodimer-1 in PBS 1×. hBMSC–scaffold constructs were washed a second time before observation under a Leica DMRXA fluorescent microscope (Leica Microsystems). The absence of non-specific reaction of the Live/Dead cell viability assay was evaluated using BCP particles or GBs without cells.

2.5. Real-time RT–PCR

Real-time RT–PCR was used to evaluate the relative level of genes characteristic of osteoblastic commitment. Briefly, hBMSCs from the three different donors were cultured on BCP particles, GBs or BCP discs. Cells cultured on plastic dishes at the same seeding density of 15 000 cells/cm^2 were used as control. After 1, 4, 7, 14 and 21 days, 3D constructs and cells cultured on plastic were washed in PBS 1× before being transferred to a 1.5 ml tube with lysis buffer and vigorously shaken to lyse the cells. Total RNA was extracted with use of an RNA extraction kit (Qiagen, Venlo, The Netherlands) according to the manufacturer's instructions. Thereafter, RNA samples (1 μg) were reverse-transcribed with the use of avian myeloblastosis virus-reverse transcriptase and random primers in a total volume of 25 μl. Real-time quantitative PCR was performed in the Chromo4 System (Bio-Rad Laboratories, Hercules, CA, USA) with SYBR Green detection and Taq DNA polymerase according to the manufacturer's recommendations. PCR amplification involved 39 cycles of 30 s at 98 °C, 15 s at 95 °C and 30 s at 60 °C. Expression of the target gene was normalized to that of the endogenous control glyceraldehyde 3-phosphate dehydrogenase (*GAPDH*). The $2^{-\Delta\Delta CN}$(cycle threshold) method was used to calculate relative expression levels, as previously described (Livak and Schmittgen, 2001). Primer sequences are listed in Table 2.

2.6. Immunohistochemistry

After 14 days of culture, cells cultured on BCP particles or GBs were removed from culture. For comparison purposes, hBMSCs cultured on plastic for 14 days were also stained for bone proteins. Before staining, hBMSC–scaffold constructs were frozen in liquid nitrogen and embedded in Tissue-Tek® OCT™ Compound (Sakura, Villeneuve d'Ascq, France). To study the expression of different proteins, 7 μm thick sections were cut with use of a cryostat microtome (Leica Cryocut 3000, Leica Microsystems Wetzlar, Germany) and stained by use of an immunohistochemistry kit (EnVision® + Dual Link System–HRP (DAB$^+$), Dako, Trappes, France). Slides were rinsed in PBS (1×) for 5 min before the endogenous enzymes were blocked for 10 min with the Dual endogenous enzyme block reagent. Samples were then washed (washing buffer, PBS 1×, 3% bovine serum albumin) before incubation with the primary antibody for 1 h at room temperature. Antibodies for the following were diluted as follows: bone morphogenetic protein 2 (BMP-2; Abcam) 1:200; collagen type I (ColI; Sigma-Aldrich) 1:4000; bone sialoprotein (BSP, Abcam) 1:600; and osteocalcin (OCN, R&D Systems) 1:200. For BMP-2, washing buffer was supplemented with 0.2% Triton (Sigma-Aldrich) for cell membrane permeation. Subsequently, samples were rinsed with washing buffer and then incubated for 30 min with labelled polymer–horseradish peroxidase. Then the slides were washed before incubation with substrate-chromogen solution for 10 min. Samples were finally mounted with use of aqueous mounting medium. Immunohistochemistry staining was assessed with positive (human bone chips) and negative controls (human cartilage; data not shown). Furthermore, the absence of non-specific staining was confirmed using BCP particles or GBs without cells (data not shown).

2.7. *In vivo* study

All animal procedures were performed in accordance with a protocol approved by the local committee for animal care and ethics. Immunocompromised mice, Swiss nude mice (female, 7 weeks old) were purchased from a professional breeder (Charles River Laboratory, France). Animals were placed in groups of five per cage inside HEPA-filtered isolators, with food and water given *ad libitum* for a 14 day quarantine before surgery. As previously described, hBMSCs from one donor were loaded at 4.5×10^5 cells onto 35 mg BCP particles or GBs (15 000 cell/cm^2). Alternatively, 7×10^5 hBMSCs were seeded onto macroporous BCP discs (surface of ~46 cm^2) at a comparable seeding density of 15 000 cells/cm^2. Cells were cultured for 7 days on these materials using

Table 2. Primers used for real time reverse transcriptase-polymerase chain reaction

Primer	Sequence (5′–3′)	PCR product length (nt)
Human *GAPDH*/left primer	agccacatcgctcagacac	66
Human *GAPDH*/right primer	gcccaatacgaccaaatcc	
Human *Runx2*/left primer	ggcccacaaatctcagatcgtt	184
Human *Runx2*/right primer	cactggcgctgcaacaagac	
Human *BMP-2*/left primer	aggacctggggaagcagcaa	117
Human *BMP-2*/right primer	gctctttcaatggacgtgtccc	
Human *ColI*/left primer	acatggaccagcagactggca	153
Human *ColI*/right primer	tcactgtcttgccccaggct	
Human *BSP*/left primer	cgaatacacgggcgtcaatg	109
Human *BSP*/right primer	gtagctgtactcatcttcataggc	
Human *OCN*/left primer	ggcgctacctgtatcaatgg	106
Human *OCN*/right primer	tcagccaactcgtcacagtc	

DOI: 10.1002/term

ultra-low-attachment plates with proliferation or osteogenic medium. The medium was refreshed every 3 days. Then hBMSC–scaffolds constructs ($n = 5$ per type of scaffold and per culture medium) were implanted subcutaneously in the backs of 23 Swiss nude mice (two implants/mouse). As negative controls, BCP particles, GBs and BCP discs were implanted without cells ($n = 5$/group). The animals were under general anaesthesia with isoflurane gas (Halothane, Baxter, Zurich, Switzerland), and the surgery was performed under aseptic conditions. Two 1 cm incisions were made along each side of the dorsum, then blunt dissection was performed to separate the skin from the subcutaneous connective tissue and form pockets under the skin, into which constructs were inserted. The skin was closed with biodegradable sutures (Monocryl 4/0 Ethicon, Johnson&Johnson, USA). After 8 weeks, animals were anaesthetized and euthanized by intracardiac injection of an overdose of sodium pentobarbital (0.5 ml; Dolethal, Vetoquinol, Lure, France). The implants were retrieved by dissection and immediately placed in fixative (neutral 4% formaldehyde) for 2 days.

2.8. Histology

Explants were processed for non-decalcified histology according to standard procedures. After fixation, samples were dehydrated in a graded series of ethanols, acetone, impregnated in methylmethacrylate and finally embedded in polymethylmethacrylate resin. After polymerization, 25 μm thick cross-sections of the samples were cut using a diamond-saw microtome (Leica SP 1600, Leica Microsystems), using the method described by van der Lubbe *et al.* (1988). Then the sections were stained with methylene blue and basic fuchsine and observed by light microscopy (Leica Microsystems).

2.9. Bone quantification

Newly formed bone within each explant was quantified using back-scattered electron microscopy (BSEM). Sections of the explants were polished and gold sputter-coated. Contiguous BSEM images were taken at × 30 magnification and 15 kV by use of an electron microscope (Leo 1450 VP, Carl Zeiss, Oberkochen, Germany). Mineralized bone and the implanted scaffolds were easily distinguished on the basis of their respective electronic densities. For each explant, two sections at different heights were analysed. The occurrence of bone formation was first determined. For bone quantification, the region of interest corresponding to the overall fibrous tissue capsule was first selected. Then, the surface of mineralized bone tissue, scaffold and non-mineralized tissue was determined using an image analysis system (QWin, Leica Microsystems). The percentage of bone was calculated by dividing the surface of mineralized bone by the available surface (total surface without surface occupied by the biomaterial) within the region of interest.

2.10. Statistical analysis

Data are expressed as mean ± standard error of the mean (SEM). Statistical analysis was performed using SPSS (Chicago, IL, USA) v 16.0 software. The non-parametric Kruskal–Wallis test was used to compare groups. Differences were considered statistically significant at $p < 0.05$.

3. Results

3.1. 3D constructs

As shown in Figure 1, BCP particles and GBs have similar shape and size but different surface microstructures. The BCP particle showed microporosity, whereas GBs exhibited a smooth surface (Figure 1a, f). After seeding, hBMSCs adhered identically on BCP particles and GBs. As shown in Figure 1b, g, similar hybrid constructs were obtained on both BCP particles and GBs after 1 day of culture. At high SEM magnification (Figure 1c, h), cells were attached by pseudopodia on multiple adjacent BCP particles or GBs. Over 4 culture days, the BCP particles or GBs moved closer to each other and resulted in a compact structure, thus reducing the construct areas while increasing their thickness. After 7 culture days, the constructs were firm and could be handled with tweezers. After 10 culture days, SEM revealed that hBMSCs synthesized an abundant ECM around and between the BCP particles or GBs, which resulted in thick cell-synthesized 3D constructs (Figure 1d, i). Similar structures were observed after 21 days of culture (Figure 1e, j).

3.2. Cell proliferation on scaffolds

Human BMSCs were capable of adhering to BCP particles or GBs and could proliferate on these substrates (Figure 2). The cells proliferated rapidly during the first 4 days and in a more slow but steady fashion over 14 days on both scaffolds. These proliferation rates were followed by a slight decrease in cell number until day 21. The ability of the two substrates to support hBMSC proliferation was further confirmed by Live/Dead cell viability assays. A minimal number of dead cells were observed on BCP particles and GBs from the first day (Figure 2b, e) until day 21 of culture (Figure 2d, g), without apparent an difference between proliferation and differentiation medium. The number of living cells on BCP particles or GBs increased over 7 days (Figure 2c, f, respectively). Furthermore, the cells presented an elongated shape characteristic of hBMSCs in expansion phase.

3.3. *In vitro* osteoblastic differentiation

As shown in Figure 3, 3D constructs formed by seeding hBMSCs on BCP particles or GBs showed an upregulation of osteoblastic markers as compared with cells cultured on BCP discs or plastic wells, regardless of the culture

DOI: 10.1002/term

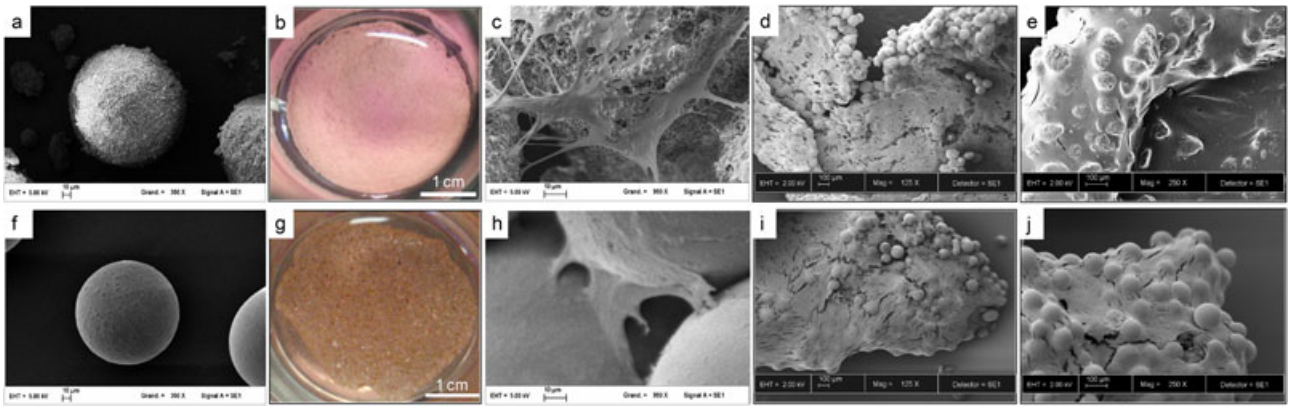

Figure 1. Formation of 3D constructs with biphasic calcium phosphate (BCP) particles (a–e) or glass beads (GBs; f–j): (a, f) SEM images of a BCP particle and GBs without cells; (b, g) stereoscopic microscopy images of human bone marrow stromal cells (hBMSCs) after 1 day of culture on BCP particles and GBs; (c, h) high-magnification SEM image of 3D constructs after 1 day of culture, showing cells attached by pseudopodia on multiple adjacent BCP particles or GBs; (d, i) SEM images showing formation of thick 3D constructs containing abundant extracellular matrix (ECM) after 10 culture days; and (e, j) after 21culture days

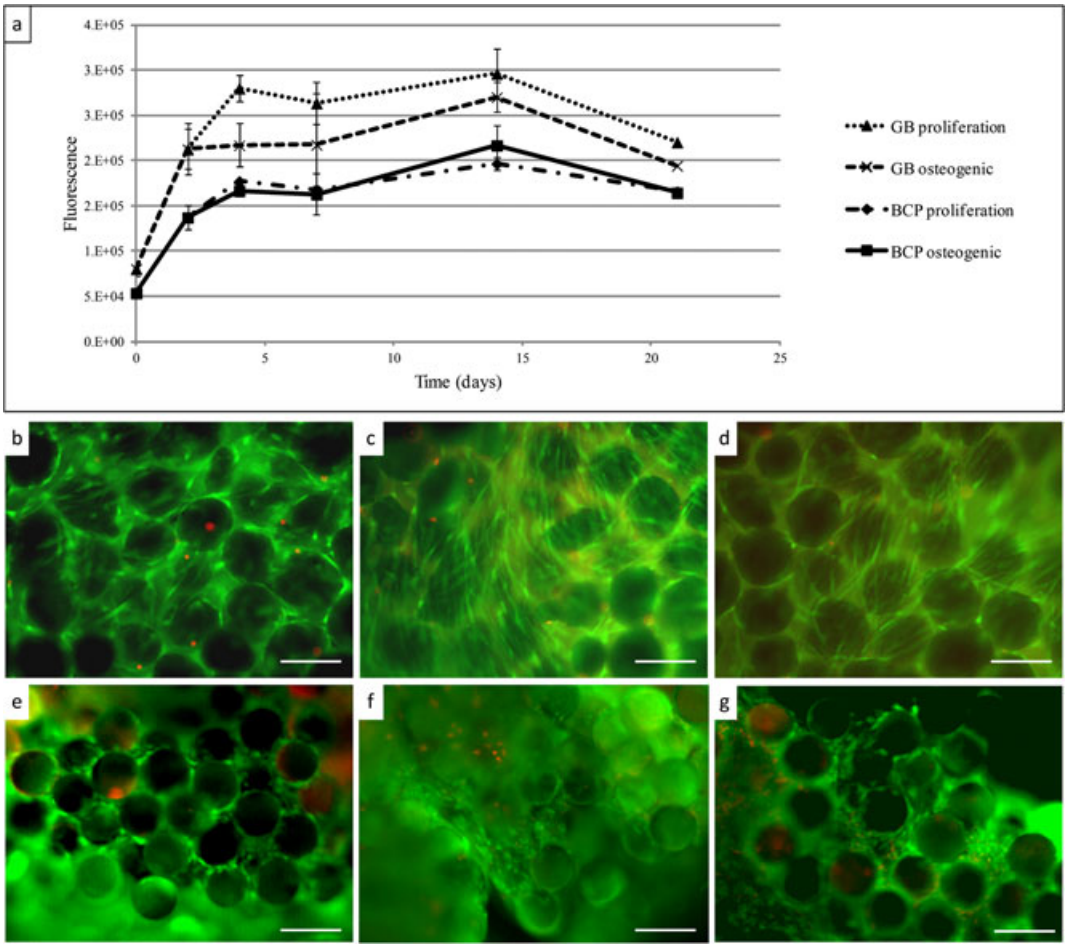

Figure 2. (a) hBMSCs proliferation on BCP particles and GBs measured by Alamar blue assay after 1, 4, 7, 14 and 21 days of culture in proliferation or osteogenic medium. Cell viability and morphology observed by LIVE/DEAD® on BCP particles (b–d) and GBs (e–g) after 1 (b, e), 7 (c, f) and 21 (d, g) days in proliferation medium. Scale bars = 200 μm

medium. Three independent experiments performed with bone marrow cells from three different donors showed similar expression profiles. Real-time RT–PCR revealed an overexpression of osteoblastic genes after 1 day of culture, except for bone sialoprotein (BSP), for which a gradual increase in expression was observed with culture time. The upregulation of *Runx2*, *BMP-2*, *Col1* and *OCN* after 1 day was followed by a lower expression level that nonetheless increased over 21 days of culture for most genes. Nevertheless, levels of expression for most of the genes were slightly higher for cells cultured on GBs than on BCP particles, notably during the initial expression peak.

DOI: 10.1002/term

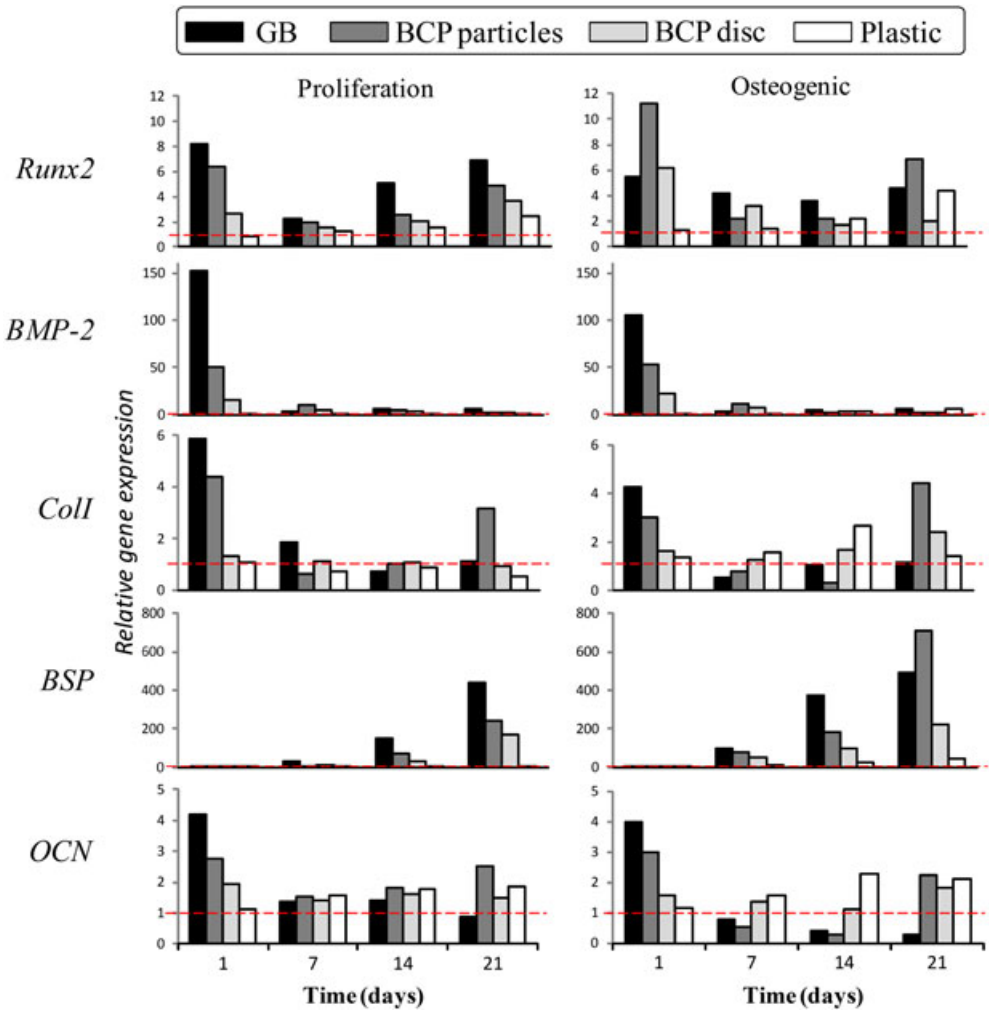

Figure 3. Real-time RT–PCR analysis of mRNA expression of osteoblastic markers (*Runx2*, *BMP-2*, *ColI*, *BSP*, *OCN*) for hBMSCs cultured on GBs, BCP particles and discs in comparison to plastic in proliferation medium (left panels) or osteogenic medium (right panels) at different times (1, 7, 14 and 21 days). Relative gene expression normalized for hBMSCs at day 0 on plastic (dashed red line). Graphs are representative of three independent experiments performed with bone marrow cells from different donors

Interestingly, the expression profiles and magnitudes were similar overall for cells cultured on BCP particles, discs or GBs in either proliferation medium or osteogenic differentiation medium. Corroborating the observed abundant ECM production, the expression of *Col1* was high after 1 day of culture on both BCP particles and GB scaffolds, while it remained initially low on plastic and BCP discs. The addition of osteogenic factors in the culture medium generally increased the expression of osteoblatic genes on plastic. However, it remained lower and delayed as compared to cells cultured on BCP particles or GBs scaffolds.

Immunohistochemistry was used to confirm, at protein level, the gene expression profiles in terms of hBMSC osteoblastic differentiation. As shown in Figure 4, osteoblastic proteins were produced by cells cultured on 3D scaffolds, such as BCP particles or GBs, even without osteogenic factors. For instance, early BMP-2, ColI, late BSP and OCN osteoblastic proteins were observed in the cell-synthesized 3D environments. Immunostaining for ColI was greater than for any other evaluated protein. Similar protein expression was observed for cells cultured on the two scaffolds. The addition of osteogenic factors to the culture medium did not change the production of bone proteins when cells were cultured on either BCP particles or GBs (see Supporting information, Figure S1). In contrast, cells cultured for 14 days on plastic produced osteoblastic proteins only in the presence of osteogenic factors.

3.4. *In vivo* implantation of cell-synthesized 3D constructs

After 8 weeks of subcutaneous implantation in nude mice, none of the different scaffolds without cells induced bone formation and were encapsulated by fibrous tissue (data not shown). As shown in Figure 5, hBMSC–BCP particle constructs induced abundant bone formation. Mineralized bone tissue was formed through all the constructs (5/5) cultured in proliferation medium for 7 days before implantation. BCP particles were surrounded by newly formed bone and bone bridges appeared between particles, as well as osteocyte lacunae. Bone quantification analysis by BSEM confirmed histological observations and showed important bone formation for cell-synthesized

DOI: 10.1002/term

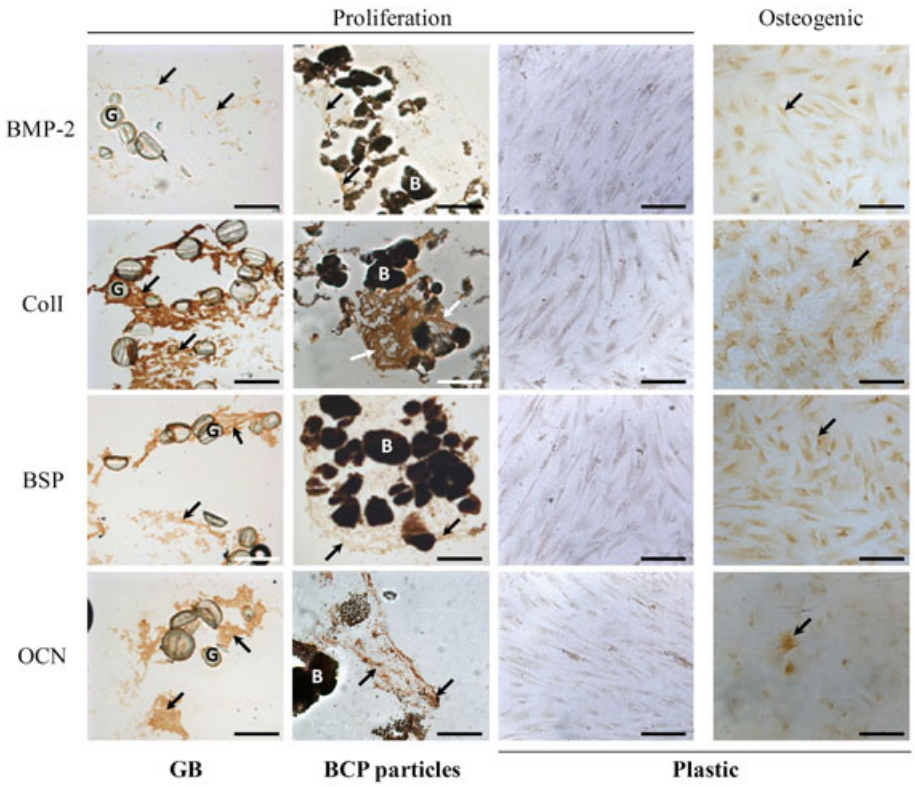

Figure 4. Immunohistological staining of BMP-2, ColI, BSP and OCN for hBMSCs cultured for 14 days on GBs (G) and BCP particles (B) in comparison to plastic in proliferation or osteogenic media. Arrows indicate positive staining of proteins. Scale bars = 300 μm

3D environments produced without osteogenic factors (Figure 6). Indeed, > 35% of the available space between BCP particles was filled with mature bone. Supplementing the culture medium with osteogenic factors also resulted in a bone occurrence of 5/5 (see Supporting information, Figure S2). However, bone formation was restrained to the periphery of samples and the quantity was lower than for previous constructs obtained in proliferation medium. For comparison, hBMSC–macroporous BCP discs induced the formation of bone. However, the amount of newly formed bone within these explants was low and not significantly different, whether the seeded scaffolds were cultured in proliferation or osteogenic medium for 7 days before implantation. Furthermore, bone formation was limited to the outer surface of the porous BCP discs (Figure 5c, d). Indeed, only 4% and 2% of bone was quantified in the macropores of BCP discs for hBMSCs cultured with or without osteogenic factors, respectively. Regarding the GBs constructs, no bone was formed in any of the implanted samples (0/5) (Figures 5e, 6). The GBs appeared to be closely packed and surrounded by fibrous tissue. Overall, the cell-synthesized 3D environment produced by BCP particles without osteogenic medium was the best condition to form bone in an ectopic site *in vivo*.

4. Discussion

Our study investigated the role of scaffolds on the osteoblastic differentiation of hBMSCs *in vitro* and the possible correlation with bone formation *in vivo*. A classical approach in bone tissue engineering consists of seeding and culturing hBMSCs on macroporous CaP scaffolds. In a comparative study, Arinzeh *et al*. (2005) demonstrated that macroporous BCP ceramics containing a high amount of TCP, viz. 20/80 HA/TCP blocks ($3 \times 3 \times 3$ mm), loaded for 2 h with 5×10^6 hBMSCs, induced the greatest amount of bone after 6 and 12 weeks in the subcutis of nude mice. Although a semi-quantitative method was used in their study, the quantity of ectopic bone was limited to the outer pores of the BCP ceramic. In our study, we obtained similar results by seeding 7.5×10^5 hBMSCs on macroporous BCP discs (diameter 8×3 mm) and culturing for 7 days prior to implantation. As shown in Figure 5, bone only formed in the outer pores of the macroporous BCP discs (4% and 2%, respectively, for constructs prepared in proliferative and osteogenic conditions, without a statistically significant difference). These small amounts of bone formation may be explained by a limited cellular penetration in the centre of the ceramic during seeding or subsequent culture, or by an insufficient vascularization due to a poor interconnectivity. Another explanation may be related to the conditions of culture of hBMSCs on the macroporous scaffold. At the cellular level, the ceramic pores are a 2D surface, while bone tissue has a 3D architecture favouring cell–cell and cell–ECM interactions. Interestingly, scaffolds made of particles provided an inverted open macroporosity favourable to oxygen and nutrient diffusion *in vitro*, as well as host cell invasion and blood vessel ingrowth *in vivo*. As schematically illustrated in Figure 7, the intergranular spaces between

DOI: 10.1002/term

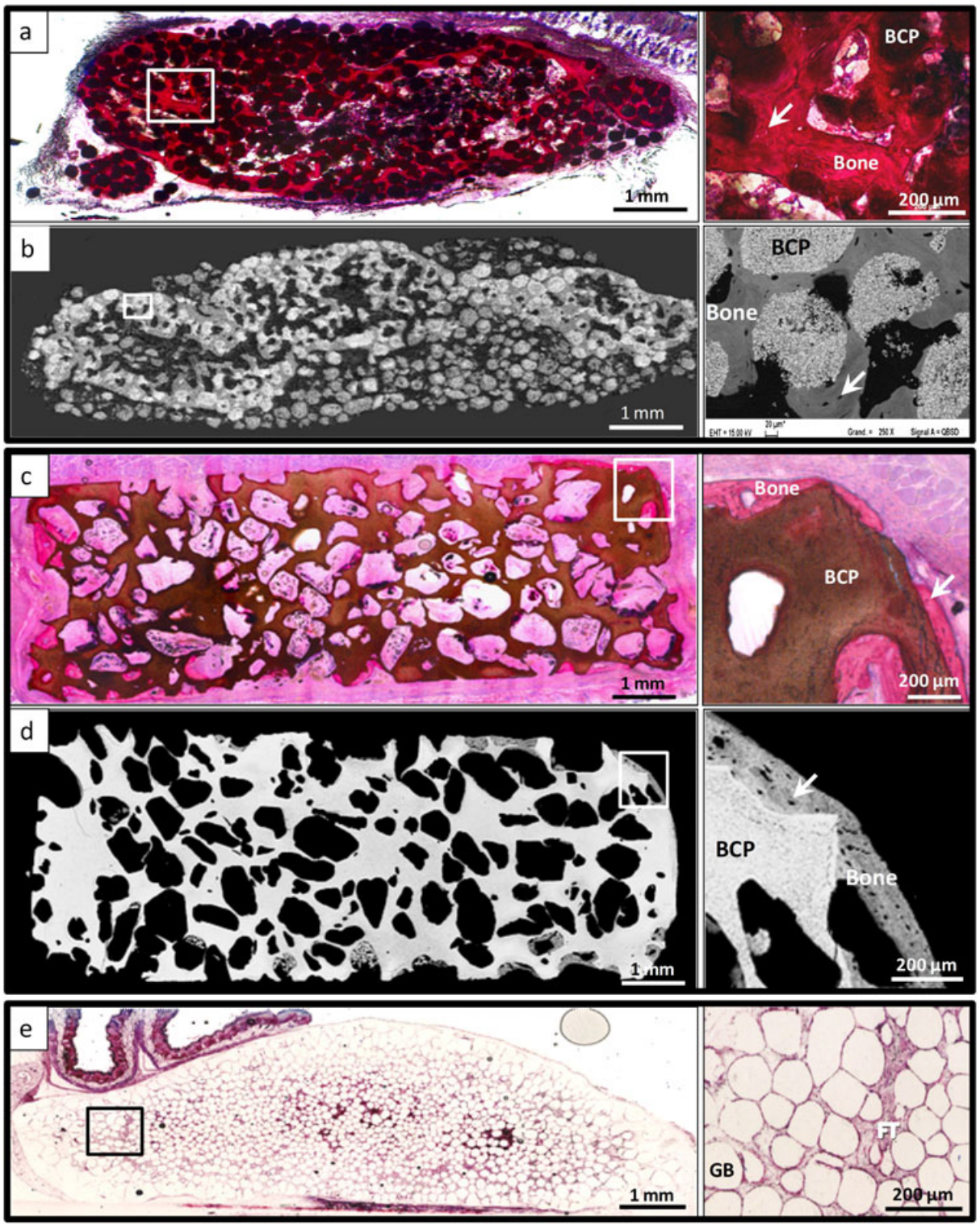

Figure 5. Histology of 3D constructs cultured *in vitro* for 7 days and implanted in the subcutis of nude mice for 8 weeks. (a, b) hBMSC–BCP particles; (c, d) hBMSC–BCP discs; (e) hBMSC–GBs: (left panels) entire explants in non-decalcified resin (basic fuchsine and toluidine blue staining) and BSEM images; (right panels) high-magnification histology and BSEM pictures. Note the mineralized bone formation with osteocytes lacunae (arrows) in contact to BCP particles and BCP discs (histology, purple; BSEM, grey). hBMSC–GBs constructs only exhibited fibrous tissue (FT) encapsulation

the particles provide an important negative porosity template readily available for the cells, as compared with traditional macroporous scaffolds. The effect of this structural difference on cells is clearly illustrated by the higher gene expression observed on BCP particles and glass beads as compared to BCP discs, especially at early culture times. Various studies have highlighted the potential of such an approach for bone formation, using ceramic

DOI: 10.1002/term

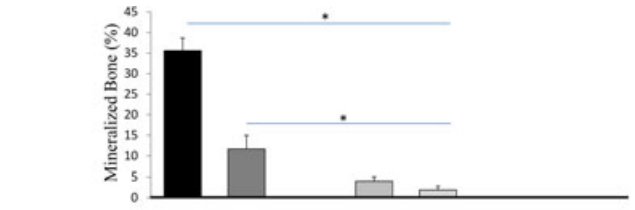

	BCP particles		BCP dises		GB	
Bone occurrence	5/5	5/5	5/5	5/5	0/5	0/5
Bone formation (%)	35.6 ± 3	11.7 ± 3	3.9 ± 0.9	1.9 ± 1	0	0

Figure 6. Quantification of mineralized bone formation in hBMSC–BCP particles, hBMSC-BCP discs and hBMSC–GB constructs obtained by culturing cells in proliferative and osteogenic media for 7 days and implanted in the subcutis of nude mice for 8 weeks. Bone occurrence and percentages of bone in the available space are indicated in the table (*$p < 0.05$)

particles or powders of different compositions and sizes (Krebsbach *et al*., 1997; Kuznetsov *et al*., 2008; Mankani *et al*., 2008; Zannettino *et al*., 2010). For instance, Mankani *et al*. (2008) investigated the effect of BCP carrier size on bone formation; they found that HA/TCP particles of 0.1–0.25 mm size demonstrated the greatest bone formation at both 4 and 10 weeks. In their study, cells were seeded at very high densities (up to 5×10^6/40 mg particles) and implanted in animal models without a prior culture step. On the other hand, Fischer *et al*. (2003) cultured goat bone marrow cells on ceramic HA particles for 7 days in osteogenic medium prior to implantation; they observed the formation of 3D constructs *in vitro*, leading to abundant bone formation *in vivo*. However, the effects of osteoblastic differentiation of hBMSCs or ECM production were not studied in these previous reports. We observed here that hybrid constructs of hBMSCs cultured on BCP particles of 0.14–0.20 mm for 7 days in proliferation medium formed abundant bone in the subcutis of nude mice. Interestingly, *in vitro* gene expression analysis of hBMSCs within these constructs indicated a spontaneous induction of the cells towards the osteoblastic lineage, without the use of osteogenic factors. In the present study, we observed similar *in vitro* osteoblastic differentiation for hBMSCs either cultured on BCP particles or GBs having comparable sizes. Indeed, hBMSCs were able to adhere to proliferate and synthesize abundant ECM on both scaffolds. SEM analysis during the first culture days further showed that hBMSCs were able to bridge the interspaces between adjacent BCP particles by multiple attachment sites or by cell–cell contact from individual particle surfaces (Figure 1c). This observation is well in agreement with previous reports showing the ability of human osteoblasts to form bridges across large gaps (> 100 μm) between poly(lactic-co-glycolic acid) microspheres (Borden *et al*., 2003). Over the culture time, in addition to cellular proliferation, ECM was synthesized around and between both types of particles, BCP or GBs, which resulted in thick cell-synthesized 3D constructs (Figure 1d, e, i, j). Intergranular spaces between the particles offer a fully open porosity, a high degree of freedom and a large surface area for the cells to proliferate in 3D and produce an abundant ECM. Interestingly, while osteoblastic differentiation was obtained on plastic with only osteogenic medium culture, spontaneous osteoblastic differentiation at the mRNA and protein levels was observed for both BCP particles and GBs (Figures 3, 4). The osteoblastic genes increased in expression during early and/or late culture, with similar patterns for both particle types. Although BCP particles and GBs differ by surface microporosity and chemistry, similar results were obtained independently with regard to cell-synthesized matrix and osteoblastic differentiation. Therefore, the spontaneous differentiation of hBMSCs into an osteoblastic lineage seems linked to the cell-synthesized 3D environment but not to the intrinsic scaffolds properties. This was further emphasized by the expression increase of most osteogenic markers after 1 day of culture, which underlines the immediate effect induced by the formation of 3D constructs. Of particular interest, genes of early transcription (*Runx2*) and growth factors (*BMP-2*) were highly overexpressed after only 1 day of culture. These two proteins are of primary importance for osteoblastic commitment and osteoblast maturation. BMP-2 activates Smads pathways

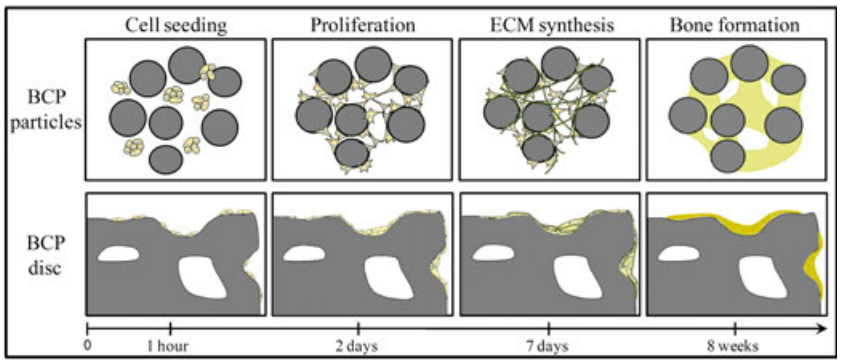

Figure 7. Schematic representation of hBMSC–BCP particles and hBMSC–BCP disc constructs as a function of time *in vitro* and *in vivo*. Cells attached on BCP 1 h after seeding, proliferated in between BCP particles (3D) or on the surface of BCP discs (2D), produced abundant extracellular matrix (ECM) in BCP particles but a small amount on BCP discs after 4–7 days and formed a large quantity of mineralized bone with trabeculae between BCP particles and a small amount on BCP discs after 8 weeks under the skin of nude mice

DOI: 10.1002/term

that act on osteoblastic gene expression via first *Runx2* and then *osterix*, which in turn act on the synthesis of proteins such as ColI, BSP and OCN (Chen *et al*., 1997; Shirakawa *et al*., 2006; Javed *et al*., 2009). The osteoblastic phenotype was further corroborated by positive immunohistological staining of early markers such as BMP2 and ColI and late markers such as BSP and OCN, similarly for each type of particle.

Different hypotheses can be formulated to explain this early osteoblastic differentiation of hBMSCs on both BCP particles and GBs. It is possible that cell–cell contact observed in the constructs plays a determinant role in this spontaneous differentiation. Indeed, a high number of cellular interactions are known to favour hBMSC osteoblastic differentiation (Li *et al*., 1999; Schiller *et al*., 2001). Moreover, the number of cell–cell interactions is potentially higher with our 3D culture conditions than with 2D culture, as illustrated in Figure 7. The spontaneous osteogenic differentiation could also be enhanced by the abundant ECM formation, which favours hBMSC proliferation and differentiation (Liu *et al*., 2004a, 2004b; Cool and Nurcombe, 2005; Valarmathi *et al*., 2008). This ECM, mainly composed of ColI, could induce proliferation of cells, which in turn continue to synthesize ECM until a certain degree of cellular confluence and ECM density is reached. At this point, hBMSCs stop proliferating and start to differentiate into an osteoblastic lineage to prepare for ECM mineralization.

In vivo, in contrast to macroporous BCP scaffolds that induce little amount of bone (Arinzeh *et al*., 2005), hBMSC–BCP particles constructs induced an abundant bone formation (up to 35% of the available space), while the hBMSC–GB constructs failed to form any bone (Figures 5, 6). Contrarily to the *in vitro* results, these observations emphasize the crucial role of BCP intrinsic properties in bone formation (Fellah *et al*., 2006; Habibovic and de Groot, 2007). Therefore, both BCP properties and the specific 3D environment are important for inducing abundant bone tissue formation in the hBMSC–BCP particle construct. BCP ceramics are known to be bioactive because of their balance between a stable HA and a more soluble TCP phase (de Groot, 1980; Shimazaki and Mooney, 1985; Hollinger and Battistone, 1986; Klein *et al*., 1994), particularly in the ratio of 20% HA:80% TCP (Arinzeh *et al*., 2005). This specific composition is soluble and gradually dissolves in the body, thereby releasing calcium and phosphate ions (Heughebaert *et al*., 1988; Daculsi *et al*., 1989, 1990; Jung *et al*., 2010). This process can be coupled with co-precipitation (Liu *et al*., 2001, 2004a, 2004b) or adsorption (Keselowsky *et al*., 2004, 2005) of proteins such as BMPs that favour bone formation *in vivo* (Yuan *et al*., 1998). Furthermore, the ion release leads to the formation of apatite microcrystals (Rohanizadeh *et al*., 1998). During bone formation, after ECM deposition, mature osteoblasts transfer extracellular calcium to nucleation sites located on collagen fibres, thus resulting in a crystal formation and mineralized matrix. ECM proteins such as ColI and BSP possess calcium-binding sites and OCN can favour calcium binding (Clarke, 2008). Consequently, calcium ions released by BCP particles in the cell-synthesized constructs could contribute to explain the abundant bone we observed *in vivo*. Ion release associated with the high amount of ECM present before implantation and the expression of key proteins could favour the rapid mineralization of the matrix after implantation and subsequent abundant bone formation. This hypothesis is supported by macroporous BCP discs that did not permit the synthesis of abundant ECM and therefore result in limited bone deposition, mainly at the location of cell seeding on the outer pores. For glass beads, the lack of calcium and phosphate release might hamper this mineralization and therefore the formation of bone. Another explanation of the absence of bone formation with hBMSC–GB constructs may be related to mechanical stresses encountered by cells under the skin of nude mice. The GBs having a smoother surface than the microporous BCP particles, the mechanical interlocking between BCP particles may be greater, even though similar constructs had formed *in vitro*. It is well known that mechanical stresses are detrimental to bone formation and more favourable to fibrous tissue (Park *et al*., 1998; Palomares *et al*., 2009). This shear stress may lead to the dedifferentiation of osteoprogenitor cells obtained *in vitro* into fibroblastic cells *in vivo* for the hBMSC–GB and not for the hBMSC–BCP particle constructs.

Interestingly, from the *in vivo* results obtained from hBMSC–BCP particle constructs, this study also indicates that the culture of constructs in osteoblastic differentiation medium prior to implantation does not result in a more important bone formation as compared to proliferation medium. This observation is surprising, as *in vitro* differentiation is commonly used in bone engineering and will require further investigation, notably focusing on the quantity and quality of synthesized ECM in the function of culture conditions.

Finally, this study highlights the difficulty of predicting *in vivo* performance of bone engineering based on *in vitro* assays. Indeed, the positive *in vitro* osteoblastic differentiation observed for hBMSC–GB constructs contrasts drastically with the lack of resulting *in vivo* bone formation. Therefore, a positive expression of osteoblastic markers *in vitro* is not sufficient and should always be comforted by *in vivo* evaluation.

5. Conclusion

The formation of hybrid 3D constructs by culturing hBMSCs on BCP particles prior to implantation is an interesting approach for bone engineering. Particles can provide a good environment for hBMSCs to proliferate and synthesize their own ECM in a cell-synthesized 3D construct. *In vitro*, this 3D environment can spontaneously induce osteoblastic commitment without the need for osteogenic factors, and *in vivo*, hBMSC–BCP particle 3D constructs form abundant, mature bone

DOI: 10.1002/term

tissue. These results highlight the importance of BCP properties and a specific 3D environment for inducing abundant bone tissue formation. In terms of clinical applications, these hBMSC–BCP constructs, leading to abundant bone formation with a relatively low number of cells, short culture time (7 days) and good handling properties may be of high interest for bone reconstruction purposes. These hybrid constructs may be used to stabilize non-union fractures, to repair large bone defects or to improve implant integration, instead of using autologous bone grafts.

Acknowledgements

The authors are grateful to Paul Pilet for valuable scientific discussions and the institution microscopy department for micro-analysis and micro-characterization (U791, LIOAD, Nantes Microscopy). The authors thank the department of Cryopréservation, Distribution, Typage et Archivage Animal (CDTA, CNRS, Orléans, France) for housing the mice, and Dr Cécile Frémond for her precious help. This work was supported by the French National Research Agency (ATOS project) and partially funded by the Directorate-General for Research of the European Commission (Grant No. 241879) through the REBORNE project.

Supporting information on the internet

The following supporting information may be found in the online version of this article:

Figure S1. Immunohistological staining of BMP-2, ColI, BSP and OCN for hBMSCs cultured for 14 days on GBs and BCP particles in osteogenic medium.

Figure S2. Histology of 3D constructs cultured in vitro for 7 days in osteogenic medium and implanted in the subcutis of nude mice for 8 weeks.

References

Arinzeh TL, Tran T, McAlary J, *et al*. 2005; A comparative study of biphasic calcium phosphate ceramics for human mesenchymal stem cell-induced bone formation. *Biomaterials* **26**(17): 3631–3638.

Borden M, El-Amin SF, Attawia M, *et al*. 2003; Structural and human cellular assessment of a novel microsphere-based tissue engineered scaffold for bone repair. *Biomaterials* **24**(4): 597–609.

Brown KL, Cruess RL. 1982; Bone and cartilage transplantation in orthopaedic surgery. A review. *J Bone Joint Surg Am* **64**(2): 270–279.

Bruder SP, Jaiswal N, Ricalton NS, *et al*. 1998; Mesenchymal stem cells in osteobiology and applied bone regeneration. *Clin Orthop Relat Res* **355**(suppl): S247–256.

Burchardt H. 1987; Biology of bone transplantation. *Orthop Clin North Am* **18**(2): 187–196.

Chen D, Harris MA, Rossini G, *et al*. 1997; Bone morphogenetic protein 2 (BMP-2) enhances BMP-3, BMP-4, and bone cell differentiation marker gene expression during the induction of mineralized bone matrix formation in cultures of fetal rat calvarial osteoblasts. *Calcif Tissue Int* **60**(3): 283–290.

Clarke B. 2008; Normal bone anatomy and physiology. *Clin J Am Soc Nephrol* **3**(suppl 3): S131–139.

Cool SM, Nurcombe V. 2005; Substrate induction of osteogenesis from marrow-derived mesenchymal precursors. *Stem Cells Dev* **14**(6): 632–642.

Cordonnier T, Langonne A, Sohier J, *et al*. 2011; Consistent osteoblastic differentiation of human mesenchymal stem cells with bone morphogenetic protein 4 and low serum. *Tissue Eng Part C Methods* **17**(3): 249–259.

Cordonnier T, Layrolle P, Gaillard J, *et al*. 2010; 3D environment on human mesenchymal stem cells differentiation for bone tissue engineering. *J Mater Sci Mater Med* **21**(3): 981–987.

Daculsi G, LeGeros RZ, Heughebaert M, *et al*. 1990; Formation of carbonate-apatite crystals after implantation of calcium phosphate ceramics. *Calcif Tissue Int* **46**(1): 20–27.

Daculsi G, LeGeros RZ, Nery E, *et al*. 1989; Transformation of biphasic calcium phosphate ceramics *in vivo*: ultrastructural and physicochemical characterization. *J Biomed Mater Res* **23**(8): 883–894.

Damien CJ, Parsons JR. 1991; Bone graft and bone graft substitutes: a review of current technology and applications. *J Appl Biomater* **2**(3): 187–208.

de Groot K. 1980; Bioceramics consisting of calcium phosphate salts. *Biomaterials* **1**(1): 47–50.

Delorme B, Charbord P. 2007; Culture and characterization of human bone marrow mesenchymal stem cells. *Methods Mol Med* **140**: 67–81.

Derubeis AR, Cancedda R. 2004; Bone marrow stromal cells (BMSCs) in bone engineering: limitations and recent advances. *Ann Biomed Eng* **32**(1): 160–165.

Fellah BH, Weiss P, Gauthier O, *et al*. 2006; Bone repair using a new injectable self-crosslinkable bone substitute. *J Orthop Res* **24**(4): 628–635.

Fischer EM, Layrolle P, van Blitterswijk CA, *et al*. 2003; Bone formation by mesenchymal progenitor cells cultured on dense and microporous hydroxyapatite particles. *Tissue Eng* **9**(6): 1179–1188.

Friedenstein AJ, Gorskaja JF, Kulagina NN. 1976; Fibroblast precursors in normal and irradiated mouse hematopoietic organs. *Exp Hematol* **4**(5): 267–274.

Habibovic P, de Groot K. 2007; Osteoinductive biomaterials – properties and relevance in bone repair. *J Tissue Eng Regen Med* **1**(1): 25–32.

Helm GA, Dayoub H, Jane JA Jr. 2001; Bone graft substitutes for the promotion of spinal arthrodesis. *Neurosurg Focus* **10**(4): E4.

Heughebaert M, LeGeros RZ, Gineste M, *et al*. 1988; Physicochemical characterization of deposits associated with HA ceramics implanted in nonosseous sites. *J Biomed Mater Res* **22**(suppl 3): 257–268.

Hollinger JO, Battistone GC. 1986; Biodegradable bone repair materials. Synthetic polymers and ceramics. *Clin Orthop Relat Res* **207**: 290–305.

Ito Y, Tanaka N, Fujimoto Y, *et al*. 2004; Bone formation using novel interconnected porous calcium hydroxyapatite ceramic hybridized with cultured marrow stromal stem cells derived from Green rat. *J Biomed Mater Res A* **69**(3): 454–461.

Javed A, Afzal F, Bae JS, *et al*. 2009; Specific residues of RUNX2 are obligatory for formation of BMP2-induced RUNX2–SMAD complex to promote osteoblast differentiation. *Cells Tissues Organs* **189**(1–4): 133–137.

Johnson KD, Frierson KE, Keller TS, *et al*. 1996; Porous ceramics as bone graft substitutes in long bone defects: a biomechanical, histological, and radiographic analysis. *J Orthop Res* **14**(3): 351–369.

Jung GY, Park YJ, Han JS. 2010; Effects of HA released calcium ion on osteoblast differentiation. *J Mater Sci Mater Med* **21**(5): 1649–1654.

Keselowsky BG, Collard DM, Garcia AJ, *et al*. 2004; Surface chemistry modulates focal adhesion composition and signaling through changes in integrin binding. *Biomaterials* **25**(28): 5947–5954.

Keselowsky BG, Collard DM, Garcia AJ. 2005; Integrin binding specificity regulates biomaterial surface chemistry effects on cell differentiation. *Proc Natl Acad Sci USA* **102**(17): 5953–5957.

Klein C, de Groot K, Chen W, *et al*. 1994; Osseous substance formation induced in porous calcium phosphate ceramics in soft tissues. *Biomaterials* **15**(1): 31–34.

Krebsbach PH, Kuznetsov SA, Satomura K, *et al*. 1997; Bone formation *in vivo*: comparison of osteogenesis by transplanted mouse and human marrow stromal fibroblasts. *Transplantation* **63**(8): 1059–1069.

Kuznetsov SA, Huang KE, Marshall GW, *et al*. 2008; Long-term stable canine mandibular augmentation using autologous bone marrow stromal cells and hydroxyapatite/tricalcium phosphate. *Biomaterials* **29**(31): 4211–4216.

Langer R, Vacanti JP. 1993; Tissue engineering. *Science* **260**(5110): 920–926.

LeGeros RZ. 2002; Properties of osteoconductive biomaterials: calcium phosphates. *Clin Orthop Relat Res* **395**: 81–98.

Li Z, Zhou Z, Yellowley CE, *et al*. 1999; Inhibiting gap junctional intercellular communication alters expression of differentiation markers in osteoblastic cells. *Bone* **25**(6): 661–666.

Liu G, Hu YY, Zhao JN, *et al*. 2004a; Effect of type I collagen on the adhesion, proliferation, and osteoblastic gene expression of bone marrow-derived mesenchymal stem cells. *Chin J Traumatol* **7**(6): 358–362.

Liu Y, Hunziker EB, Layrolle P, *et al*. 2004b; Bone morphogenetic protein 2 incorporated into biomimetic coatings retains its biological activity. *Tissue Eng* **10**(1–2): 101–108.

Liu Y, Layrolle P, de Bruijn J, *et al*. 2001; Biomimetic coprecipitation of calcium phosphate and bovine serum albumin on titanium alloy. *J Biomed Mater Res* **57**(3): 327–335.

Livak KJ, Schmittgen TD. 2001; Analysis of relative gene expression data using real-time quantitative PCR and the $2^{-\Delta\Delta C_T}$ method. *Methods* **25**(4): 402–408.

Mankani MH, Kuznetsov SA, Marshall GW, *et al*. 2008; Creation of new bone by the percutaneous injection of human bone marrow stromal cell and HA/TCP suspensions. *Tissue Eng Part A* **14**(12): 1949–1958.

Nair MB, Suresh Babu S, Varma HK, *et al*. 2008; A triphasic ceramic-coated porous hydroxyapatite for tissue engineering application. *Acta Biomater* **4**(1): 173–181.

Okamoto M, Dohi Y, Ohgushi H, *et al*. 2006; Influence of the porosity of hydroxyapatite ceramics on *in vitro* and *in vivo* bone formation by cultured rat bone marrow stromal cells. *J Mater Sci Mater Med* **17**(4): 327–336.

Oklund SA, Prolo DJ, Gutierrez RV, *et al*. 1986; Quantitative comparisons of healing in cranial fresh autografts, frozen autografts and processed autografts, and allografts in canine skull defects. *Clin Orthop Relat Res* **205**: 269–291.

Palomares KT, Gleason RE, Mason ZD, *et al*. 2009; Mechanical stimulation alters tissue differentiation and molecular expression during bone healing. *J Orthop Res* **27**(9): 1123–1132.

Park SH, O'Connor K, McKellop H, *et al*. 1998; The influence of active shear or compressive motion on fracture-healing. *J Bone Joint Surg Am* **80**(6): 868–878.

Petite H, Viateau V, Bensaid W, *et al*. 2000; Tissue-engineered bone regeneration. *Nat Biotechnol* **18**(9): 959–963.

Pittenger MF, Mackay AM, Beck SC, *et al*. 1999; Multilineage potential of adult human mesenchymal stem cells. *Science* **284**(5411): 143–147.

Prockop DJ. 1997; Marrow stromal cells as stem cells for nonhematopoietic tissues. *Science* **276**(5309): 71–74.

Reed JS. 1995; *Principles of Ceramics Processing*, 2nd edn. Wiley Interscience: New York.

Ripamonti U. 1996; Osteoinduction in porous hydroxyapatite implanted in heterotopic sites of different animal models. *Biomaterials* **17**(1): 31–35.

Rohanizadeh R, Padrines M, Bouler JM, *et al*. 1998; Apatite precipitation after incubation of biphasic calcium-phosphate ceramic in various solutions: influence of seed species and proteins. *J Biomed Mater Res* **42**(4): 530–539.

Schiller PC, D'Ippolito G, Balkan W, *et al*. 2001; Gap-junctional communication is required for the maturation process of osteoblastic cells in culture. *Bone* **28**(4): 362–369.

Shimazaki K, Mooney V. 1985; Comparative study of porous hydroxyapatite and tricalcium phosphate as bone substitute. *J Orthop Res* **3**(3): 301–310.

Shirakawa K, Maeda S, Gotoh T, *et al*. 2006; CCAAT/enhancer-binding protein homologous protein (CHOP) regulates osteoblast differentiation. *Mol Cell Biol* **26**(16): 6105–6116.

Sun H, Ye F, Wang J, *et al*. 2008; The upregulation of osteoblast marker genes in mesenchymal stem cells prove the osteoinductivity of hydroxyapatite/tricalcium phosphate biomaterial. *Transpl Proc* **40**(8): 2645–2648.

Urist MR, Strates BS. 1970; Bone formation in implants of partially and wholly demineralized bone matrix. Including observations on acetone-fixed intra- and extracellular proteins. *Clin Orthop Relat Res* **71**: 271–278.

Vaccaro AR. 2002; The role of the osteoconductive scaffold in synthetic bone graft. *Orthopedics* **25**(suppl 5): s571–578.

Valarmathi MT, Yost MJ, Goodwin RL, *et al*. 2008; A three-dimensional tubular scaffold that modulates the osteogenic and vasculogenic differentiation of rat bone marrow stromal cells. *Tissue Eng Part A* **14**(4): 491–504.

van der Lubbe HB, Klein CP, de Groot K. 1988; A simple method for preparing thin (10 μM) histological sections of undecalcified plastic embedded bone with implants. *Stain Technol* **63**(3): 171–176.

Yamasaki H, Sakai H. 1992; Osteogenic response to porous hydroxyapatite ceramics under the skin of dogs. *Biomaterials* **13**(5): 308–312.

Yuan H, Zou P, Yang Z, *et al*. 1998; Bone morphogenetic protein and ceramic-induced osteogenesis. *J Mater Sci Mater Med* **9**(12): 717–721.

Zannettino AC, Paton S, Itescu S, *et al*. 2010; Comparative assessment of the osteoconductive properties of different biomaterials *in vivo* seeded with human or ovine mesenchymal stem/stromal cells. *Tissue Eng Part A* **16**(12): 3579–3587.